THE JOURNAL OF BIOLOGICAL CHEMISTRY
Vol. 279, No. 50, Issue of December 10, pp. 51888–51896, 2004
Printed in U.S.A.

P–O Bond Destabilization Accelerates Phosphoenzyme Hydrolysis of Sarcoplasmic Reticulum Ca^{2+}-ATPase*

Received for publication, July 29, 2004
Published, JBC Papers in Press, September 27, 2004, DOI 10.1074/jbc.M410867200

Andreas Barth‡§ and Natalya Bezlyepkina¶

From the ‡Department of Biochemistry and Biophysics, The Arrhenius Laboratories for Natural Sciences, Stockholm University, S-106 91 Stockholm, Sweden, and the ¶Institut für Biophysik, Johann Wolfgang Goethe-Universität, D-60590 Frankfurt am Main, Germany

The phosphate group of the ADP-insensitive phosphoenzyme (E2-P) of sarcoplasmic reticulum Ca^{2+}-ATPase (SERCA1a) was studied with infrared spectroscopy to understand the high hydrolysis rate of E2-P. By monitoring an autocatalyzed isotope exchange reaction, three stretching vibrations of the transiently bound phosphate group were selectively observed against a background of 50,000 protein vibrations. They were found at 1194, 1137, and 1115 cm^{-1}. This information was evaluated using the bond valence model and empirical correlations. Compared with the model compound acetyl phosphate, structure and charge distribution of the E2-P aspartyl phosphate resemble somewhat the transition state in a dissociative phosphate transfer reaction; the aspartyl phosphate of E2-P has 0.02 Å shorter terminal P–O bonds and a 0.09 Å longer bridging P–O bond that is ~20% weaker, the angle between the terminal P–O bonds is wider, and −0.2 formal charges are shifted from the phosphate group to the aspartyl moiety. The weaker bridging P–O bond of E2-P accounts for a 10^{11}–10^{15}-fold hydrolysis rate enhancement, implying that P–O bond destabilization facilitates phosphoenzyme hydrolysis. P–O bond destabilization is caused by a shift of noncovalent interactions from the phosphate oxygens to the aspartyl oxygens. We suggest that the relative positioning of Mg^{2+} and Lys^{684} between phosphate and aspartyl oxygens controls the hydrolysis rate of the ATPase phosphoenzymes and related phosphoproteins.

Phosphorylation is one of the fundamental regulatory mechanisms in biology (1). It also governs the catalytic mechanism of the sarcoplasmic reticulum Ca^{2+}-ATPase (SERCA1) (2), where it controls the ordered sequence of catalytic steps to ensure the efficiency of the overall catalytic reaction. Here we study one of the ATPase phosphoenzyme intermediates by monitoring an enzyme-catalyzed isotopic exchange reaction at the phosphate group with infrared spectroscopy. The result is an infrared spectrum at "atomic resolution" in a crowded spectral region. It observes selectively the transiently bound phosphate group, a group that cannot be studied by site-directed mutagenesis. Our approach can be extended to other phosphoproteins and reveals here the molecular cause of an important property of the phosphoenzyme studied.

The Ca^{2+}-ATPase (2) pumps two Ca^{2+} ions against a concentration gradient across the sarcoplasmic reticulum membrane, which relaxes a flexed muscle (for reviews see Refs. 3–8). The energy for this active transport process is provided by the substrate ATP, which phosphorylates the ATPase at Asp^{351} to form at least two consecutive phosphoenzymes, Ca_2E1-P and E2-P. The Ca^{2+} transport step is associated with the conversion from Ca_2E1-P to E2-P. These phosphoenzymes have different catalytic properties; while the first phosphoenzyme intermediate Ca_2E1-P dephosphorylates with ADP to reform ATP, the second phosphoenzyme E2-P reacts with water. This switch of catalytic specificity ensures the efficiency of the pump process, because the specificity of Ca_2E1-P is such that the energy provided by ATP is not wasted before Ca^{2+} is transported. After Ca^{2+} transport, E2-P hydrolyzes remarkably faster than the model compound acetyl phosphate in water. The time constant for E2-P hydrolysis is between 10 and 100 ms near 25 °C depending on the pH (9–12), whereas that of acetyl phosphate is 10^5 s (25 °C, pH 6.8) (13). This 10^6–10^7-fold acceleration of the reaction by the enzyme is essential for the fast progression of the pump cycle and therefore for the efficient removal of Ca^{2+} from the cytoplasm.

Obviously, the environment of the phosphate group is important in controlling the dephosphorylation properties. It has been found to become more hydrophobic in the transition from Ca_2E1-P to E2-P (14, 15), and this seems to account for an increased hydrolysis rate of E2-P as compared with Ca_2E1-P (Ref. 16; reviewed in Ref. 17). The molecular mechanism of dephosphorylation has, however, not been elucidated.

We were interested in how the environment of the phosphate group controls its catalytic properties and used infrared spectroscopy to study the phosphate group of E2-P in detail. Infrared spectroscopy has proved valuable for the investigation of protein catalysis (18–24) because it allows measurement of interaction strengths and bond lengths at a level of sensitivity that exceeds even that of x-ray crystallography and NMR (25).

Since the early days of infrared spectroscopy on proteins, the power of selective isotopic labeling has been exploited to observe a specific group in a large protein (26, 27). Because of the mass effect on vibrational frequencies, infrared absorption bands of a labeled group are shifted with respect to those of the unlabeled group and can be identified in the spectrum. Specific labeling is usually necessary to identify a specific group in the spectrum, because otherwise the absorption of this group will be hidden under the overwhelming absorption of other groups. For the investigation of protein reactions, another necessity in most cases is the use of reaction-induced infrared difference spectroscopy, where the reaction of interest is started in the infrared cuvette. We release a biological compound of interest from a biologically inactive photosensitive precursor (caged

* This work was supported by Deutsche Forschungsgemeinschaft Grant Ba1887/4-1. The costs of publication of this article were defrayed in part by the payment of page charges. This article must therefore be hereby marked "*advertisement*" in accordance with 18 U.S.C. Section 1734 solely to indicate this fact.

§ To whom correspondence should be addressed. Tel.: 46-8-162452; Fax: 46-8-155597; E-mail: Andreas.Barth@dbb.su.se.

compounds), for example ATP from caged ATP[1] (Ref. 28; reviewed in Ref. 29). By calculating the difference between the infrared absorption before and after start of the reaction, only those groups are detected that participate actively; the absorption of the vast majority of passive groups cancels.

Here we combine and extend both approaches to observe selectively the phosphate group of E2-P; [γ-$^{18}O_3$]ATP released from [γ-$^{18}O_3$]caged ATP transfers the labeled γ-phosphate to the ATPase, which then accumulates a labeled E2-P phosphoenzyme under appropriate experimental conditions. This phosphoenzyme catalyzes an isotopic exchange with water at the phosphate oxygens (9, 30), which can be observed with infrared spectroscopy. Isotopically labeled caged compounds were used before in experiments on the Ca^{2+}-ATPase (31, 32) and on Ras (33–35). They were evaluated by a careful comparison or subtraction of spectra obtained with labeled and unlabeled compounds. This approach has proved to be of limited sensitivity for detecting the E2-P phosphate vibrations (36). The approach here is to combine selective labeling of a protein with the induction of an autocatalyzed isotopic exchange (36). Thus we obtain directly a difference spectrum between labeled and unlabeled E2-P in a single time-resolved experiment. We observe selectively three stretching vibrations of the phosphate group of a protein with nearly 50,000 normal modes of vibration. The vibrational frequencies identified reveal a shift of electron density from the P–O bond that connects protein and phosphate to the terminal P–O bonds. This weakens the link to the protein and accelerates hydrolysis of E2-P. The approach used here to study one of the Ca^{2+}-ATPase phosphoenzymes can be extended to other phosphoenzymes, if necessary with the help of auxiliary proteins to induce phosphorylation or dephosphorylation.

EXPERIMENTAL PROCEDURES

Time-resolved Fourier transform infrared measurements were performed at 10 °C, and the samples were prepared as described previously (37). They contained ~0.9 mM Ca^{2+}-ATPase, 100 mM imidazole buffer, pH 6.5, 5 mM caged ATP, 200 μM Ca^{2+}, 20 mM Mg^{2+}, 5 mM dithiothreitol, 0.5 mg/ml Ca^{2+} ionophore A23187, 1 mg/ml adenylate kinase, 10% Me_2SO. All of the spectra were normalized to an identical protein concentration using the amide II absorbance (31).

Correlation of Vibrational Frequency with Bond Valence—Deng *et al.* (38) have defined a fundamental frequency for the stretching vibration for phosphates, which for PO_3^{2-} is $\nu = [(\nu_s^2 + 2\nu_{as}^2)/3]^{1/2}$, with ν_s and ν_{as} being the symmetric and asymmetric stretching vibrations of the terminal P–O bonds, respectively. The frequency of the asymmetric stretching vibration is weighted by a factor of 2 because this vibration is doubly degenerate. The fundamental frequency is less dependent on the geometry of the phosphate group than the asymmetric and symmetric stretching vibrations of the terminal P–O bonds themselves (38). We slightly extend the approach by Deng *et al.* to phosphate groups in asymmetric environments by defining the fundamental frequency as follows: $\nu = [(\nu_1^2 + \nu_2^2 + \nu_3^2)/3]^{1/2}$ where ν_1, ν_2, and ν_3 are the frequencies of the terminal P–O bonds that we have observed for the E2-P phosphoenzyme. In this equation three different frequencies appear for the three terminal P–O vibrations because the degeneracy of the asymmetric stretching vibrations is lifted by the asymmetric environment of the E2-P phosphate group. The fundamental frequency can be used to calculate the bond valence of P–O bonds using the following formula (38),

$$s = [0.175 \times \ln(224500\ \mathrm{cm}^{-1}/\tilde{\nu})]^{-4.29} \quad \text{(Eq. 1)}$$

where s is the bond valence in vu, and $\tilde{\nu}$ is the wavenumber that corresponds to the fundamental frequency. In our case, where the phosphate group is in an asymmetric environment, the bond valence s represents the average bond valence of the three terminal P–O bonds. The bond valence of the bridging P–O bond was calculated by subtracting the summed bond valences of the terminal P–O bonds from 5, the atomic valence of phosphorus. The average bond valence of external bonds (noncovalent bonds to the environment) to the terminal phosphate oxygens was calculated by subtracting the average bond valence of the terminal P–O bonds from 2, the atomic valence of oxygen.

Correlation of Bond Valence with Bond Length—Bond valences can be derived from bond lengths in such a way that they sum up to the atomic valence within a few percentages (39) for a large number of oxides. We used Equation 2 (40) with the parameters (41) used to derive the frequency *versus* bond valence correlation (Equation 1) (38),

$$s = L_1^N/L_s^N \quad \text{(Eq. 2)}$$

where s is the bond valence measured in vu, L_s is the bond length of a bond with bond valence s, and L_1 is the bond length of a bond with a bond valence of 1 vu. L_1 and N are constants for a given type of bond (39, 41): $N = 4.29$, and $L_1 = 1.622$ Å for P–O bonds (41). Bond lengths determined differed by 0.01 Å (0.6%) or less from those determined with the exponential expression and more recent parameters from Ref. 40.

It should be noted that the values given in Table I for bond lengths and bond valences should not be considered to be accurate to three digits after the decimal point. Three digits are given to avoid rounding errors when the differences between acetyl phosphate and E2-P are discussed.

RESULTS

To observe isotope exchange at the E2-P phosphate group, E2-P was prepared by the release of ATP from caged ATP in the absence of K^+ and the presence of Me_2SO and Ca^{2+} ionophore, which are conditions that accumulate E2-P as discussed and shown in previous work (37, 42). This work also established a marker band for E2-P near 1194 cm^{-1} that was later assigned to the phosphate group (32). In the present work, sample conditions and temperature were fine-tuned so that the E2-P concentration is constant over several minutes. During that time the ATPase dephosphorylates and rephosphorylates several times leading to oxygen exchange between water and phosphate group (30). If water and phosphate oxygen isotopes are different, an isotope exchange at the E2-P phosphate group is the consequence of oxygen exchange that can be followed by infrared spectroscopy (36). Several isotope exchange experiments were performed using [γ-$^{16}O_3$]caged ATP in [^{18}O]water, [γ-$^{18}O_3$]caged ATP in [^{16}O]water, [γ-$^{18}O_1$]caged ATP in [^{16}O]water, and [γ-$^{18}O_1$]caged ATP in [^{18}O]water. Control samples contained [γ-$^{16}O_3$]caged ATP in [^{16}O]water or [γ-$^{18}O_3$]caged ATP in [^{18}O]water.

Fig. 1 shows infrared difference spectra of E2-P formation from Ca_2E1 (Ca_2E1 → E2-P) in which the E2-P spectrum was recorded before and after isotope exchange. The bold line spectra were recorded before isotope exchange, and the thin line spectra were recorded afterward. The spectra overlap well above 1300 cm^{-1} where phosphates do not absorb, which confirms that the E2-P concentration is constant during the experiment. Below 1300 cm^{-1}, spectra before and after exchange differ because of band shifts that are the result of the isotope exchange reaction.

The spectra in Fig. 1*a* were obtained with unlabeled caged ATP in [^{18}O]H_2O, and the first, bold spectrum is characteristic of [$^{16}O_3$]E2-P as indicated by the marker band at 1194 cm^{-1} (32). Within 3 min, this band decays because of isotope exchange at the phosphate group, and the thin line spectrum is obtained. The absorbance changes associated with isotope exchange are very small. This is expected because they are caused by frequency shifts of the terminal P–O stretching vibrations which account for 3 vibrations of 50,000 protein vibrations.

The isotope exchange experiment shown in Fig. 1*b* was carried out in the reverse direction; the ATPase was phosphorylated with [γ-$^{18}O_3$]caged ATP, which produced [$^{18}O_3$]E2-P first and [$^{16}O_3$]E2-P after oxygen exchange with [^{16}O]H_2O. Consequently the first spectrum (*bold line*) shows only a small signal

[1] The abbreviations used are: caged ATP, P^3-1-(2-nitrophenyl)ethyl ATP; vu, valence unit(s).

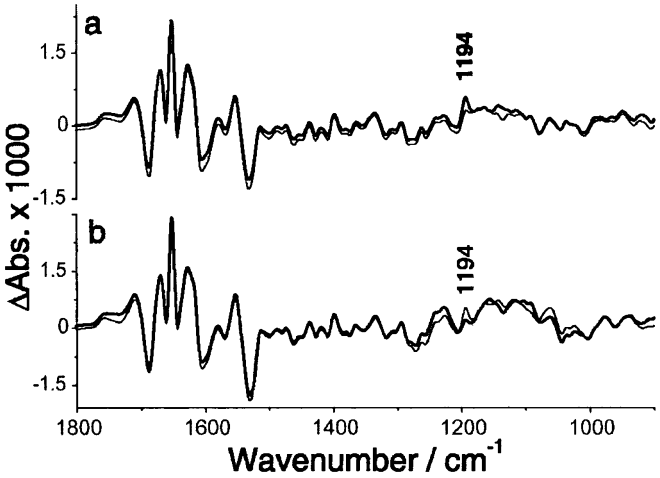

FIG. 1. **Infrared difference spectra of the reaction $Ca_2E1 \rightarrow$ E2-P before and after oxygen isotope exchange at the phosphate group.** Difference spectra were calculated by subtracting a reference spectrum recorded before the photolysis flash from spectra recorded between 7 and 28 s (*bold line*, spectrum before exchange) and between 97 and 195 s (*thin line*, spectrum after exchange) after the flash. *a*, spectra obtained with [γ-$^{16}O_3$]caged ATP in [^{18}O]H_2O (12 experiments from 3 samples). *b*, spectra obtained with [γ-$^{18}O_3$]caged ATP in [^{16}O]H_2O (13 experiments from 4 samples).

at 1194 cm^{-1}, which has increased in the thin line spectrum after isotope exchange. The comparison of the spectra in *panels a* and *b* of Fig. 1 demonstrate the excellent reproducibility of the infrared difference spectra.

To show the isotope exchange associated absorbance changes more clearly, the bold and thin line spectra of Fig. 1 were subtracted. The spectra obtained are shown in Fig. 2 and are named isotope exchange spectra. Fig. 2*a* shows the $^{16}O_3 \rightarrow {}^{18}O_3$ exchange spectrum, with positive bands being caused by [$^{18}O_3$]E2-P and negative bands being caused by [$^{16}O_3$]E2-P. The featureless spectrum above 1300 cm^{-1} demonstrates again that the E2-P concentration is constant to a very high degree in this experiment. In addition to bands caused by isotope exchange, other reactions might contribute to the spectrum. To distinguish these bands from isotope exchange bands, the exchange experiment was performed in the reverse direction ($^{18}O_3 \rightarrow {}^{16}O_3$), which should lead to a mirror image spectrum when compared with that in Fig. 2*a*.

Fig. 2*b* shows two of these $^{18}O_3 \rightarrow {}^{16}O_3$ exchange spectra. As expected for the isotope exchange spectrum, bands appear at the same positions as in Fig. 2*a* but with the opposite sign. The spectra show also bands caused by the slow steady state hydrolysis of ATP near 1250 and 1060 cm^{-1} (28, 43). The hydrolysis rate is sensitive to the concentration of Me_2SO, which is difficult to control precisely during the preparation of infrared samples. Therefore the hydrolysis rate varied between experiments. The bold line spectrum is the average of all experiments, and the thin line spectrum is the average of experiments with slow hydrolysis. A weighted subtraction of the spectrum of all samples from the spectrum of samples with slow hydrolysis was calculated to subtract the hydrolysis bands from the exchange spectrum (data not shown). The criterion for appropriate subtraction was a flat spectrum around 1250 cm^{-1} where a strong hydrolysis band is observed. This correction did not abolish the sharp bands between 1200 and 1090 cm^{-1}, which shows that they are not associated with hydrolysis. However, the subtraction reduced the relative amplitudes of the bands below 1105 cm^{-1}. Before discussing the spectra in more detail, further controls are shown in Fig. 2*c*.

Fig. 2*c* shows several control spectra. For the two full line spectra no isotope exchange is expected because the isotopes of

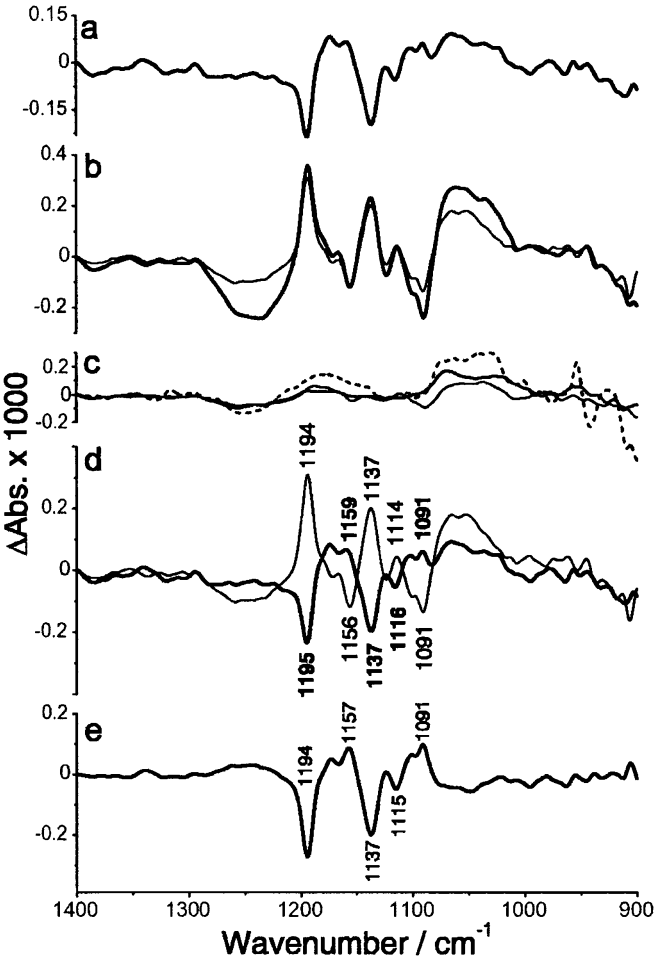

FIG. 2. **Infrared difference spectra of isotope exchange at the phosphate group.** Spectra were calculated by subtracting the spectrum before exchange from the spectrum after exchange (see Fig. 1). *a*, spectrum reflecting the absorbance changes during the reaction E2-$P^{16}O_3 \rightarrow$ E2-$P^{18}O_3$, termed $^{16}O_3 \rightarrow {}^{18}O_3$ exchange spectrum (12 experiments from 3 samples). *b*, difference spectra of the reaction E2-$P^{18}O_3 \rightarrow$ E2-$P^{16}O_3$, termed $^{18}O \rightarrow {}^{16}O$ exchange spectra. *Bold line*, spectrum averaged from all $^{18}O \rightarrow {}^{16}O$ experiments (13 experiments from 4 samples); *thin line*, spectrum averaged from experiments with low hydrolytic activity (6 experiments from 4 samples). *c*, control spectra. Spectra of experiments are shown in which no isotope exchange is expected because the oxygen isotopes of γ-phosphate of ATP and water were the same (*full lines*) or because the ATPase was inhibited by the Ca^{2+} chelator EGTA. Otherwise the conditions and data evaluation was as for spectra shown in Fig. 1. *Thin line*, control spectrum obtained with labeled ATP and labeled water (16 experiments from 4 samples); *bold line*, spectrum obtained with unlabeled ATP and unlabeled water (15 experiments from 4 samples); *Dotted line*, spectrum obtained in the presence of 20 mM EGTA upon release of [γ-$^{18}O_3$]ATP in [^{16}O]H_2O (1 experiment). *d*, comparison of $^{18}O_3 \rightarrow {}^{16}O_3$ exchange spectrum with little hydrolysis (*thin line*) and $^{16}O_3 \rightarrow {}^{18}O_3$ exchange spectrum (*bold line*). Spectra shown are those of *a* and *b*. *e*, spectrum after subtraction of absorbance changes not related to isotope exchange. The spectrum was calculated by subtracting the $^{18}O_3 \rightarrow {}^{16}O_3$ exchange spectrum from $^{16}O_3 \rightarrow {}^{18}O_3$ exchange spectrum and dividing by 2.

γ-phosphate of ATP and water are the same (^{18}O in the thin line spectrum and ^{16}O in the bold line spectrum). The *dashed line* spectrum shows an experiment where the ATPase was inhibited by the addition of the Ca^{2+} chelator EGTA. These spectra demonstrate that the sharp bands between 1200 and 1090 cm^{-1} in Fig. 2 (*a* and *b*) are only observed when the isotopes of γ-phosphate of ATP and water are different and when the ATPase is active. Therefore bands with opposite signs in Fig. 2 (*a* and *b*) are attributed to isotope exchange at the phosphate oxygens of E2-P.

These bands are easily identified in Fig. 2*d* where the isotope

exchange spectrum of Fig. 2*a* and that with slow hydrolysis of Fig. 2*b* are shown. The comparison highlights the mirror image property of the two spectra in the region between 1200 and 1090 cm^{-1}.

The mirror image property is not perfect for the amplitudes of positive bands at 1159 and 1091 cm^{-1} in the bold line spectrum. Correction for hydrolysis of the $^{18}O_3 \rightarrow {}^{16}O_3$ exchange spectrum as discussed above improved the mirror image property by reducing slightly the amplitude of the 1091-cm^{-1} band. However, we prefer to show the original data here. Another reason for the small deviation from the ideal mirror image property could be incomplete isotope exchange in one of the spectra. We think that isotope exchange is complete for the $^{18}O_3 \rightarrow {}^{16}O_3$ exchange as discussed below. However, it might not be complete for the $^{16}O_3 \rightarrow {}^{18}O_3$ exchange. In these samples, the flat spectrum around 1250 cm^{-1} indicates very slow steady state hydrolysis of ATP. Therefore, E2-P was more stable in these samples than in samples for the $^{18}O_3 \rightarrow {}^{16}O_3$ exchange with the possible consequence that isotope exchange is not complete during the observation time.

To improve further the quality of the exchange spectrum, the two spectra in Fig. 2*d* were subtracted and divided by two. This cancels contributions to the spectrum that are unrelated to isotope exchange and enhances those related to isotope exchange. The resulting spectrum is shown in Fig. 2*e*. Negative bands in this spectrum are due to [$^{16}O_3$]E2-P and are found at 1194, 1137, and 1115 cm^{-1}. Identification of [$^{18}O_3$]E2-P bands is less clear because positive bands are less prominent. The largest positive bands are observed at 1157 and 1091 cm^{-1}. We propose that upon $^{16}O_3 \rightarrow {}^{18}O_3$ exchange the band at 1194 cm^{-1} shifts to 1157 cm^{-1} and that at 1115 cm^{-1} shifts to 1091 cm^{-1}. The band at 1137 cm^{-1} likely shifts to around 1115 cm^{-1} where it partially cancels the [$^{16}O_3$]E2-P band, which explains the small amplitude of the 1115 cm^{-1} band compared with the other two [$^{16}O_3$]E2-P bands. Small bands in the spectrum can be caused by substrates of E2-P or by a small percentage of Ca_2E1-P.

As a further test for the robustness of our isotope exchange spectrum, we conducted experiments with singly labeled caged ATP, [γ-$^{18}O_1$]caged ATP, which are shown in Fig. 3*a*. The *bold line* shows the experiment in [^{16}O]water reflecting $^{18}O_1{}^{16}O_2 \rightarrow {}^{16}O_3$ exchange (absorbance of [$^{16}O_3$]E2-P minus that of [$^{18}O_1{}^{16}O_2$]E2-P), and the *thin line* shows the experiment in [^{18}O]water reflecting $^{18}O_1{}^{16}O_2 \rightarrow {}^{18}O_3$ exchange (absorbance of [$^{18}O_3$]E2-P minus that of [$^{18}O_1{}^{16}O_2$]E2-P).

A discussion of the individual band shifts in the spectra of Fig. 3*a* is beyond the scope of this work. One band, however, is worth mentioning here. Near 1195 cm^{-1}, a relatively large positive band is observed in the bold line spectrum but only a small band in the thin line spectrum. This indicates that the amplitude of this band is relatively large for [$^{16}O_3$]E2-P but small for [$^{18}O_1{}^{16}O_2$]E2-P, which therefore can be used as a marker band for complete exchange in an $^{18}O_3 \rightarrow {}^{16}O_3$ exchange experiment. The large amplitude of this band in the thin line spectrum of Fig. 2*d* demonstrates that $^{18}O_3 \rightarrow {}^{16}O_3$ exchange is complete or close to complete in this experiment.

The spectra for partial isotope exchange can be used to mathematically obtain a second spectrum for full exchange. By subtracting the two spectra, the contribution of [$^{18}O_1{}^{16}O_2$]E2-P cancels, and the absorbance of [$^{18}O_3$]E2-P minus that of [$^{16}O_3$]E2-P is obtained. This spectrum is shown as a *thin line* in Fig. 3*b* and compared with the experimental spectrum for full $^{16}O_3 \rightarrow {}^{18}O_3$ exchange from Fig. 2*e*. The match between these spectra is very good and confirms the above attribution of bands to isotope exchange.

The spectral positions of the phosphate bands are unaffected by the presence of Me_2SO in our samples; band positions in isotope exchange spectra were the same for 10–30% Me_2SO. In experiments not designed to monitor isotope exchange, the 1194 cm^{-1} band was observed at the same position in the presence and absence of Me_2SO in spectra like those shown in Fig. 1.

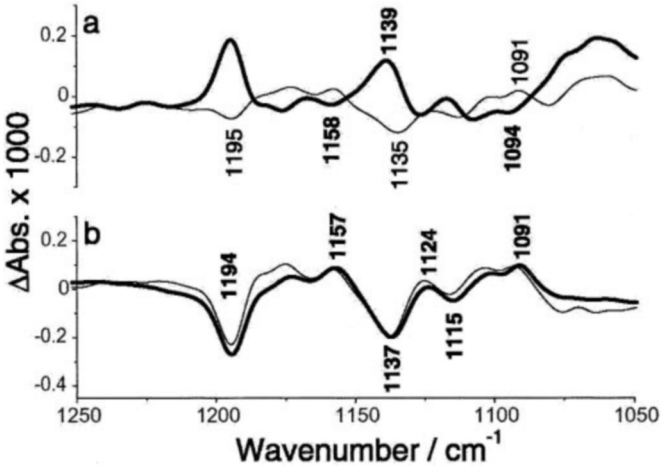

FIG. 3. **Infrared difference spectra of partial and full isotope exchange.** *a*, infrared difference spectra of partial isotope exchange at the phosphate group. The E2-P phosphate group was singly labeled by [γ-$^{16}O_2{}^{18}O_1$]caged ATP, and the experiments were conducted in ^{18}O labeled or unlabeled water. The spectra were calculated by subtracting a spectrum before exchange from one after exchange using the same time intervals as for the spectra in Figs. 1 and 2. *Bold line*, spectrum of the E2-$P^{16}O_2{}^{18}O_1 \rightarrow$ E2-$P^{16}O_3$ reaction (6 experiments from 3 samples); *thin line*, spectrum for E2-$P^{16}O_2{}^{18}O_1 \rightarrow$ E2-$P^{18}O_3$ reaction (6 experiments from 6 samples). *b*, comparison of spectra for full isotope exchange obtained either directly from the experiment or mathematically from partial exchange spectra (see text). *Bold line*, spectrum obtained from experiments of full exchange after subtraction of absorbance changes not related to isotope exchange (same as in Fig. 2*e*); *thin line*, spectrum calculated by subtracting the two partial exchange spectra shown in *a*.

DISCUSSION

Infrared Bands of the E2-P Phosphate Group—Three bands of the E2-P phosphate group have been identified: those at 1194, 1137, and 1115 cm^{-1}. They are associated with the P–O stretching vibrations of the PO_3 moiety. The spectral positions of the phosphate bands are different from those of the model substance acetyl phosphate in water, which shows only two bands at lower wavenumbers: that of the symmetric stretching vibration at 983 cm^{-1} and that of the degenerated asymmetric vibration at 1132 cm^{-1}. The observation of three bands for E2-P is due to an asymmetric environment around the phosphate group that lifts the degeneracy.

The band at 1194 cm^{-1} has been identified before as a phosphate band (32) by comparing spectra obtained with labeled and unlabeled caged ATP. It was observed at the slightly different position of 1192 cm^{-1} because Mg^{2+} was absent in these samples, but 1 mM of Ca^{2+} was present instead. Experiments with only 150 μM Ca^{2+} but 1 mM Mg^{2+} and otherwise identical conditions (data not shown) showed the band at 1194 cm^{-1} as found here at 20 mM Mg^{2+}, lower buffer concentration, and lower pH. Therefore the catalytic cation, which binds with ATP to the ATPase and remains bound at least until E2-P is hydrolyzed (44), has a direct influence on the band position of one of the phosphate bands and binds most likely directly to the aspartyl phosphate. The band is slightly narrower with Mg^{2+}, indicating less conformational freedom with the physiological ion Mg^{2+} than with Ca^{2+}.

Summary of Calculations—In the following we will use an approach outlined by Deng *et al.* (38) to calculate P–O bond

TABLE I
Properties of the E2-P phosphate group and acetyl phosphate

	E2-P phosphate group		Phosphate group of acetyl phosphate	
	Terminal oxygen	Bridging P–O	Terminal P–O	Bridging P–O
Wavenumbers of P–O stretching vibrations (cm^{-1})	1194		1132	
	1137		1132	
	1115		982	
P–O fundamental frequency or wavenumber (cm^{-1})	1149		1082	
P–O bond valence (vu)	1.409	0.772	1.343	0.972
Bond valence of external bonding (formal charge) (vu)	0.591		0.657	
P–O bond length (Å)	1.497	1.723	1.514	1.633
P–O force constant (10^2 nm^{-1})	7.8	3.4	7.4	4.8

strengths, P–O bond lengths, and finally the dissociation energy of the bridging P–O bond. The general line of calculations can be summarized as follows. From the observed terminal P–O vibrational frequencies, we calculate their average P–O bond strengths or more specifically their average bond valence. From this, the bond valence of the bridging P–O bond can be derived, because the sum of all bond valences around phosphorus is 5. Bond valences can be correlated with bond lengths and these with force constants. The latter two can be related to the dissociation energy of the bridging P–O bond, and this can be used to estimate the decrease in activation energy and the increase in dephosphorylation rate that is achieved by enzymatic catalysis. Further correlations will be exploited to calculate the average angle between bridging P–O bond and terminal P–O bonds.

Introduction to Bond Valence—The bond valence model is based on the classical chemical concept of valence. It ascribes an *atomic valence* to each atom, which can be thought of as the number of electrons participating in chemical bonding. To each bond is assigned a *bond valence*, s, in valence units (vu), which is a measure of bond strength and can be regarded as the number of electron pairs associated with a bond. The *valence sum rule* states that the sum of bond valences equals the atomic valence. The concept of valence bond strength was originally developed by Pauling (45) for ionic bonds but applies also to covalent bonds (39, 46). Because it applies to both ionic and covalent bonds, bond valence integrates covalent and ionic contributions to a bond. Bond valence is a powerful concept because it relates to many observable properties (40, 47). We will now discuss the bond parameters of the phosphate group in detail.

Bond Valences of E2-P and Acetyl Phosphate—We have calculated the bond valences of the terminal P–O bonds from the fundamental frequencies of E2-P and acetyl phosphate in water (see "Experimental Procedures"). The values, listed in Table I and Fig. 4, indicate that the enzyme environment of E2-P increases the bond valence of the terminal P–O bonds by 5% to 1.41 vu via a reduction of external bond valences by 10%. This results in a cumulative reduction of bond valence of the bridging P–O bond by 20% to 0.77 valence units. This analysis assumes that bonding to the attacking nucleophile is negligible in E2-P. If not, the bond valence of the bridging P–O bond will be even smaller than stated above. A reduction in bridging P–O bond valence leads to a corresponding increase in bond valence of the adjacent C–O bond (because the sum of the two bond valences has to equal the atomic valence of oxygen), unless the reduction of P–O bond valence is fully compensated by external bonding to the bridging oxygen. An increase in C–O bond valence will decrease the C=O bond valence to keep the sum of the bond valences around the carbon atom equal to its atomic valence of 4. These bond valence changes make the carbon-oxygen bonds more similar to the product state where they have equal bond valence.

The bond valence of the C=O bond of acetyl phosphate can be estimated to be between 1.6 and 1.7 vu from its band position in the infrared spectrum at 1718 cm^{-1} (31), correlations between wavenumber and bond length (48, 49), and correlations between bond length and bond valence (40, 41).

Bond Lengths of E2-P and Acetyl Phosphate—Table I lists bond lengths of bridging and terminal P–O bonds of E2-P and acetyl phosphate in water obtained with equation 2 (see Experimental Procedures). The terminal P–O bonds are shorter for E2-P by 1% or nearly 0.02 Å, whereas the bridging P–O bond is longer by 5% or nearly 0.09 Å. This increase indicates a weakening of the bond that bridges phosphate group and enzyme, which will be quantified in the next section.

Bond Energy of the Bridging P–O Bond of E2-P—In the following we present several estimations of the reduction of bond energy of the bridging P–O bond of E2-P with respect to that of acetyl phosphate. (i) Bond energy can be regarded as linear to bond valence (50). Accordingly the bond energy of the bridging P–O bond of E2-P is only 80% of that of acetyl phosphate. Assuming that the latter is close to a typical P–O single bond energy of 420 kJ/mol (51), the bond energy in E2-P is reduced by 86 kJ/mol with respect to that of acetyl phosphate. (ii) Bond length L and bond energy E are correlated; for several oxides, the inverse relationship $E \sim (L - L_0)^{-1}$ has been found (52), where $L_0 = 1.171$ Å for P–O bonds (53). Using this relationship, the bridging P–O bond energy of E2-P is found to be 84% of that of acetyl phosphate. Assuming again a typical value of the acetyl phosphate bond of 420 kJ/mol, the bond energy in E2-P is reduced by 68 kJ/mol with respect to that of acetyl phosphate. (iii) Further correlations between bond length L and bond energy can be made indirectly by first correlating bond length with bond force constant f and then correlating force constant with bond energy. The equation $f = 10^{(2.06\text{Å} - L/0.63\text{Å})}$ N/cm (54) with the parameters for bonds between first and second row elements (55) fits an impressive number of compounds and is used to obtain the force constants in Table I. They can be used to check the data evaluation so far by recalculating the vibrational wavenumber in the harmonic approximation. For the average terminal P–O bond wavenumber of acetyl phosphate, a value of 1085 cm^{-1} is calculated in excellent agreement with the experimental value of 1082 cm^{-1}. The dissociation energy is proportional to the vibrational frequency and therefore to the square root of the force constant, if quadratic terms are sufficient to describe the energy levels of an anharmonic oscillator, which they are for a Morse potential (56). From this we calculate that the dissociation energy of the terminal P–O bond of E2-P is reduced to 85% of the respective acetyl phosphate bond. With the P–O single bond energy of 420 kJ/mol, the bond energy of E2-P is reduced by 64 kJ/mol. (iv) Force constants can be directly correlated with bond energies (57), which gives a bond energy for the bridging P–O bond of ~400 kJ/mol for acetyl phosphate and of 310 kJ/mol for E2-P, which is about 90 kJ/mol lower and corresponds to 78% of the acetyl phosphate bond energy. The correlation used here does not include P–O bonds. Therefore the value of 90 kJ/mol is

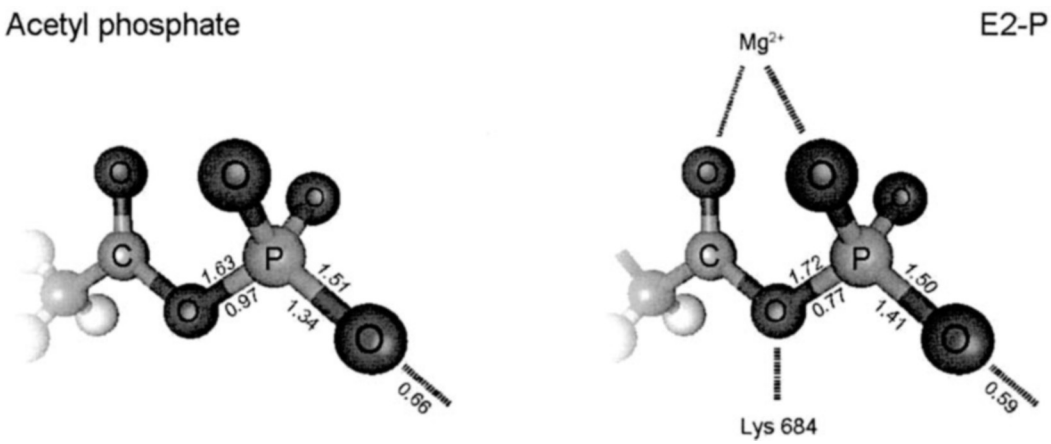

FIG. 4. **Phosphate bond parameters for acetyl phosphate and E2-P and a model for the phosphate group environment of E2-P.** The *italic numbers* above the bonds give bond lengths in Å, and the *non-italic numbers* below the bonds give bond valences in vu. Interactions of Mg^{2+} and Lys^{684} with the E2-P phosphate group are inferred from the interpretation of our spectra and protein interactions observed for aspartylphosphates (see text).

considered less reliable than those obtained by the above estimations.

Rate Enhancement of Phosphate Hydrolysis by Enzymatic Catalysis—The above considerations indicate a reduction in bond energy by about 20% of the bridging P–O bond of E2-P with respect to acetyl phosphate corresponding to 64–90 kJ/mol. Because this is the bond that is broken upon E2-P hydrolysis, the contribution of P–O bond splitting to the activation energy will be reduced by a similar amount, resulting in a dramatic 10^{11}–10^{15}-fold increase in the hydrolysis rate. This shows that P–O bond destabilization contributes significantly to the catalysis of phosphoenzyme hydrolysis.

The increase calculated is more than the observed 10^6–10^7-fold acceleration (see Introduction) likely because the rate increase caused by the lower activation energy is partly compensated by a considerable decrease of the pre-exponential factor in the Arrhenius equation. The same is observed for the model compound acetyl phosphate; the addition of organic solvents accelerates hydrolysis of acetyl phosphate by several orders of magnitude by decreasing the activation energy for hydrolysis (16). However, the rate enhancement is less than expected because the effect on the activation energy is partly counteracted by a large decrease of the pre-exponential factor. Both effects are more pronounced in the presence of Mg^{2+}; when the Me_2SO concentration is raised from 0 to 60% in the presence of 0.1 M NaOH, the activation energy decreases from 77.5 to 13.8 kJ/mol, which accelerates the rate more than 10^{11}-fold, but the pre-exponential factor decreases by 9 orders of magnitude which results in a total rate enhancement by a factor of 40 (16).

Stabilization of the E2-P Phosphate Group versus P–O Bond Destabilization—There is an apparent contradiction between the P–O bond destabilization and less external bonding to the phosphate group observed in this work and the view that the phosphate group is stabilized on E2-P (58). The latter was concluded from the observation that the free energies of free enzyme E plus phosphate and E2-P are approximately the same, whereas that of acetyl phosphate is higher than that of acetate plus phosphate. From this, a stabilization of E2-P of 50 kJ/mol (12.5 kcal/mol) has been calculated, which was ascribed to the intrinsic binding energy of the phosphate moiety of the acyl phosphate when it binds to the active site (58).

This view concentrates on the phosphate group and ascribes a rather passive role to protein and solvent. In the presence of protein conformational changes and solvent exclusion, there may be stabilizing effects that are not localized on the phosphate group (but are caused by phosphorylation). The observed stabilization of E2-P corresponds to the formation of two typical salt bridges, formation of two or three hydrogen bonds, or the transfer of two ethyl groups from water to protein (59, 60), which could take place distant from the phosphate group. Thus weaker bonding to the phosphate group may be overcompensated by stronger bonding between other groups and by entropic effects. We infer one such effect: stronger bonding to the aspartyl moiety. Whether this will overcompensate the weaker bonding to the phosphate group is difficult to conclude. Furthermore, because bond energies are only one contribution to the Gibbs free energy and because the solvent contribution is unknown, it is impossible to judge whether these local effects will stabilize the aspartyl phosphate or not in terms of free energy. In conclusion, our observation of less external bonding to the phosphate moiety of aspartyl phosphate does not contradict the observation that the phosphate group on E2-P is stabilized compared with acetyl phosphate if the total system of solvent and protein is considered.

Geometry of the E2-P Phosphate Group—The changes in bond lengths induced by the phosphate group environment will change the geometry of the phosphate group. From results on YMX_3 compounds with C_{3v} symmetry including phosphates (61), it can be inferred that an increased bridging P–O bond length makes phosphorus and terminal oxygens come closer to lie in one plane. According to the correlation for phosphates (61), the angle between bridging P–O bond and terminal P–O bonds decreases from a value of 106° for acetyl phosphate in water to 102° for the E2-P phosphate group. This holds for C_{3v} symmetry and might serve as an approximation to the "real case" of an asymmetric environment of the E2-P phosphate group. A decrease in angle between bridging and terminal P–O bonds will increase the angle between two terminal P–O bonds. This can be rationalized by increased electrostatic repulsion caused by the higher electron density in bonds with higher bond strength, in analogy to findings for PO_2^- groups on the basis of semi-empirical calculations (62). These differences in phosphate geometry between E2-P and acetyl phosphate will make the E2-P phosphate group more accessible for nucleophilic attack.

Charge Distribution on the E2-P Aspartyl Phosphate Moiety—The bond valence of external bonds can be considered as formal charges that add up for all atoms of a molecule to the total charge of the molecule (40). In calculating this sum, external bonds formed by atoms acting as anions are counted negative, and those of atoms acting as cations are counted positive (see discussion of charged and neutral molecules in

Ref. 40). The formal charge of the three terminal acetyl phosphate oxygens is $-0.657 \times 3 = -1.971$, and that of the E2-P phosphate oxygens $-0.591 \times 3 = -1.773$, *i.e.* 0.2 formal charges less negative. Because the net charge is the same (−2) for acetyl phosphate and aspartyl phosphate, the loss of negative formal charge on the terminal oxygens of E2-P must be compensated by an equal increase in negative charge or a decrease in positive charge in the aspartyl moiety. This represents a shift of negative charge away from the PO_3 group toward the aspartyl moiety of E2-P, rendering the charge distribution on the aspartyl moiety closer to the product state.

Mechanism of Phosphate Hydrolysis—Two limiting cases for phosphate transfer reactions have been discussed in the literature (1): (i) the fully associative mechanism, where the attacking nucleophile and all P–O bonds form single bonds with phosphorus in the transition state; and (ii) the fully dissociative mechanism (S_N1), where the bridging P–O bond is completely broken before a bond is formed with the attacking nucleophile and the transition state is metaphosphate-like (PO_3^-). The following properties of E2-P in comparison with those of acetyl phosphate make the ground state of E2-P resemble somewhat the transition state of a dissociative mechanism: stronger terminal P–O bonds, a weaker bridging P–O bond, less partial charge on the terminal oxygens, and a shift of charge from the phosphate moiety to the aspartyl moiety. The lengthening of the bridging P–O bond by 0.1 Å represents about 5% of the distance change required for the fully dissociative mechanism (distance larger than 3.3 Å (1)). In terms of energy, this corresponds to about 20% of the energy required to break the bond.

Is the E2-P Phosphate Environment Hydrophobic?—The averaged bond valence of all external bonds to each terminal oxygen in acetyl phosphate is 0.66 vu, which gives 0.22 vu/hydrogen bond for the ideal oxygen coordination number of four (one intramolecular bond and three extramolecular bonds) (40), which correlates well with the Lewis base strength of HPO_4^{2-} of 0.22 vu (47). This indicates that hydrogen bonds to acetyl phosphate in water are stronger than those found between water molecules (0.17 vu) (40). External bonding to the aspartyl phosphate of E2-P is reduced by 10% to 0.59 vu as compared with acetyl phosphate in water. Assuming again a coordination number of four, *i.e.* three external bonds, the typical bond valence of an external bond is close to 0.2 vu. This external bond valence between phosphate oxygens and protein is considerable because their bond valence is comparable with hydrogen bonds in ice (0.2 vu) and larger than those between water molecules (0.17 vu) (40). Therefore it does not seem appropriate to speak of a hydrophobic environment of the phosphate group, although the interactions are weakened with respect to those of acetyl phosphate in water. This weakening can be achieved by subtle changes in external bond lengths on the order of 0.1 Å according to bond valence *versus* bond length relationships (40) as discussed below.

We will now consider two scenarios for the reduction of external bonding to the terminal phosphate oxygens of E2-P with respect to acetyl phosphate in water: (i) a uniform weakening of all external bonds discussed at the example of hydrogen bonds and (ii) a weakening of one of the external bonds that accounts for the total difference in external bonding of 0.2 vu between E2-P and acetyl phosphate. In the first case, the reduction of bond valence corresponds to an increase in average hydrogen bond length. This increase is about 0.06 Å calculated by using the bond valence *versus* bond length correlation for hydrogen bonds with distances larger than 1.7 Å (40). Therefore, a slight widening of the phosphate binding cavity is sufficient to weaken the bridging P–O bond by 20%. In the second case, a loss of one hydrogen bond or a considerable weakening of a bond between a terminal oxygen and Mg^{2+} could account for the weaker external bonds in E2-P. Mg^{2+} typically forms bonds of 0.33 vu and a bond length of 2.1 Å with oxygen. An increase in bond length to 2.4 Å is sufficient to reduce the bond valence to 0.13 vu and to account for the reduction in external bonding seen for E2-P. As this discussion shows, subtle changes in external bond lengths are sufficient to weaken significantly the bridging P–O bond with a dramatic impact on the catalytic power of the enzyme.

Interactions of the Aspartyl Oxygens—Above we have discussed a shift of −0.2 formal charges from the PO_3 group to the aspartyl moiety. Because formal charge is equivalent to external bond valence, the aspartyl moiety of E2-P experiences interactions with the environment that are different from those of the acetyl moiety of acetyl phosphate. The obvious target for the main change in interactions seems to be the two oxygen atoms of the aspartyl moiety, which are expected to experience about 0.2 vu stronger external bonds in E2-P.

The external bonds to the carbonyl oxygen of E2-P will therefore be somewhat stronger than those of acetyl phosphate, which account for 0.3–0.4 vu (atomic valence of 2 minus bond valence of C=O, see above). An external bond to the bridging oxygen is suggested by the following argument: given that the bond of the bridging oxygen to the phosphorus atom has a bond valence of 0.77 vu, the C–O bond is expected to have a bond valence of 1.23 vu (2 vu − 0.77 vu) in the absence of external bonding. This is at variance with the principle of maximum symmetry, which states that bonds tend to be as symmetric as possible under the given constraints (40). To reduce the asymmetry between the two bonds, the bridging oxygen will have a tendency to form external bonds, which lowers the bond valence of the C–O bond. In line with that, protein interactions with the bridging oxygen have been found for several phosphate compounds (63–67).

The additional interaction to the aspartyl moiety accounts for about 0.2 valence units, corresponding to one additional hydrogen bond. It seems difficult to conceive that the aspartyl phosphate of E2-P should experience one hydrogen bond more than acetyl phosphate in water. Therefore it is more likely that the average external bonds to the aspartyl moiety are stronger, either because hydrogen bonds are shorter or because of interactions with ions. Interaction of the aspartyl moiety with ions is facilitated in E2-P because −0.2 formal charges are shifted from the PO_3 moiety to the aspartyl moiety. The charge on the oxygens can be compensated by Mg^{2+} and/or by Lys^{684}, which is close to Asp^{351} in the structures of the Ca^{2+}-loaded and the Ca^{2+}-deprived forms of the ATPase (68, 69). Mg^{2+} and a three coordinate NH_3^+ moiety have typical bonding strengths of 0.33 (formal charge divided by number of bonds) so they can form stronger bonds than neutral hydrogen bond donors. We suggest that Mg^{2+} and Lys^{684} interact with the aspartyl oxygens of E2-P.

The Role of Mg^{2+}—The position of Mg^{2+} seems to play a key role in determining the electron distribution on the phosphate group. The smaller bonding strength of the terminal phosphate oxygens of E2-P compared with those of acetyl phosphate destabilizes their interaction with Mg^{2+} according to the valence matching principle (40) and makes them a better match for an interaction with neutral hydrogen bond donors. In contrast, the increase in formal charge on the aspartyl oxygens in E2-P increases their bonding strengths and makes them a better match for Mg^{2+}. Thus it is conceivable that Mg^{2+} forms weaker bonds with phosphate oxygens and a stronger bond with an aspartyl oxygen. Mg^{2+} bridging a phosphate and an aspartyl oxygen of aspartyl phosphate can be expected in a protein environment because this binding mode is increasingly adopted

by the model compound acetyl phosphate when the solvent polarity is reduced (70). In the reverse reaction, phosphorylation of the Ca^{2+}-free ATPase by inorganic phosphate, such an arrangement provides a template for the reactants and catalyzes the reaction by *induced intramolecularity* (71).

Model for the Environment of the E2-P Aspartylphosphate—In the following we propose a model for the interactions of the aspartylphosphate of E2-P, which is shown in Fig. 4. According to our model Mg^{2+} bridges the carbonyl oxygen and a terminal phosphate oxygen; the side chain of Lys^{684} interacts with the bridging oxygen. In line with the important role of Lys^{684} in catalysis suggested here, it was found that this residue is crucial for enzyme phosphorylation and conversion of the ADP-sensitive phosphoenzyme Ca_2E1-P to E2-P (72). Just before this work was submitted, a new crystal structure of the ATPase was published (73) that shows for a Ca_2E1P analogue the binding mode suggested here for E2P.

A bridging cation and a Lys close to the bridging oxygen (2.8–4.0 Å N–O distance) are also found for other proteins that form an aspartyl phosphate intermediate: the receiver/phosphoacceptor domain of Spo0A (64), phosphoserine phosphatase (65), and β-phosphoglucomutase (66), with the latter two belonging to the haloacid dehalogenase superfamily as does the phosphorylation domain of the Ca^{2+}-ATPase (74). No bridging cation but a Lys 3.3 Å away from the bridging oxygen is observed for the FixJ receiver domain (67).

A cation bridging a phosphate oxygen and the carbonyl oxygen as such cannot explain the high hydrolysis rate of the Ca^{2+}-ATPase because two phosphoenzymes with that binding mode are stable enough to crystallize (64, 66). Therefore we conclude that the interactions with the aspartyl oxygens must be weaker for β-phosphoglucomutase and Spo0A than for E2-P, and the interactions with the phosphate oxygens must be stronger. Accordingly these two proteins exhibit relatively strong bonding to the phosphate oxygens and weak bonding to the aspartyl oxygens as discussed in the following. The Lys residue is relatively distant (4.0 Å) from the bridging oxygen in the β-phosphoglucomutase structure and the phosphate group points toward an open cleft with at least one of the phosphate oxygens in close contact with water molecules seen in the crystal structure (66). In the crystal structure of Spo0A, two phosphate oxygens are close to two water molecules in a cleft, and the bridging cation is Ca^{2+}, which forms a bond to the carbonyl oxygen with an estimated bond valence of only 0.2 vu (40) (based on the distance of 2.6 Å), which is weaker than those observed with Mg^{2+} in the other structures (65, 66) with estimated bond valences around 0.4 vu (based on the distance of around 2.0 Å). One of the proteins with the binding mode discussed here, phosphoserine phosphatase, was not crystallized in the phosphorylated state but with BeF_3^- as aspartyl phosphate analogue, indicating that the phosphoenzyme hydrolyzes more rapidly than β-phosphoglucomutase and Spo0A. Interestingly, this is the protein where the strongest interactions with the aspartyl oxygens are inferred from the structure: Lys is closest to the bridging oxygen (N–O distance 2.8 Å) and Mg^{2+} 2.1 Å away from the carbonyl oxygen.

The Transition between Ca_2E1-P and E2-P—We consider the above discussion of the differences between acetyl phosphate and E2-P to be a reasonable template for the changes that bring about the different chemical properties of Ca_2E1-P and E2-P. The Ca_2E1-P aspartyl phosphate seems to be in a similar environment as acetyl phosphate in water, because their carbonyl bands and their highest energy phosphate bands are found at similar wavenumbers (31). Therefore we propose that the relative strength of noncovalent bonding to the phosphate and aspartyl oxygens is one of the key factors that tunes the hydrolysis rate of the ATPase phosphoenzymes and related phosphoproteins. Weaker bonding to the phosphate oxygens and stronger bonding to the aspartyl oxygens weakens and elongates the bridging P–O bond, which increases dramatically the catalytic power of the enzyme. Elongation of the P–O bond is not accomplished by external mechanical forces acting on this bond but is an in-built response of aspartyl phosphate to a shift of interactions from phosphate to aspartyl oxygens. Shifting the relative bonding strengths can be achieved by the relative positioning of Mg^{2+} and Lys^{684} between phosphate and aspartyl oxygens with only subtle changes in distances being required. This provides an elegant "handle" for the enzyme to control hydrolysis.

Acknowledgments—We gratefully acknowledge W. Mäntele (Johann Wolfgang Goethe-Universität, Frankfurt am Main) for continuous support and provision of facilities, W. Hasselbach (Max-Planck-Institut, Heidelberg) for the gift of Ca^{2+}-ATPase, M. R. Webb (National Institute for Medical Research, London) for [γ-$^{18}O_3$]ATP, J. E. T. Corrie (National Institute for Medical Research, London) for caged ATP, and I. D. Brown (McMaster University, Hamilton, Canada) for intense and valuable discussions on the bond valence model.

REFERENCES

1. Mildvan, A. S. (1997) *Proteins* **29,** 401–416
2. Hasselbach, W., and Makinose, M. (1961) *Biochem. Z.* **333,** 518–528
3. Andersen, J. P. (1989) *Biochim. Biophys. Acta* **988,** 47–72
4. Hasselbach, W. (1981) in *Membrane Transport* (Bonting, S. L., and De Pont, J. J. H. H. M., eds) pp. 183–208, Elsevier, Amsterdam
5. Inesi, G., and de Meis, L. (1985) in *The Enzymes of Biological Membranes*, 2nd Ed., Vol. 3 (Martonosi, A., ed) pp. 157–191, Plenum Press, New York
6. Martonosi, A., Kracke, G., Taylor, K. A., Dux, L., and Peracchia, C. (1985) *Soc. Gen. Phys. Ser.* **39,** 57–85
7. Mintz, E., and Guillain, F. (1997) *Biochim. Biophys. Acta* **1318,** 52–70
8. Lee, A., and East, J. (2001) *Biochem. J.* **356,** 665–683
9. McIntosh, D. B., and Boyer, P. D. (1983) *Biochemistry* **22,** 2867–2875
10. Vieyra, A., Scofano, H. M., Guimaraes-Motta, H., Tume, R. K., and de Meis, L. (1979) *Biochim. Biophys. Acta* **568,** 437–445
11. Chaloub, R. M., Guimaraes-Motta, H., Verjovski-Almeida, S., de Meis, L., and Inesi, G. (1979) *J. Biol. Chem.* **254,** 9464–9468
12. Rauch, B., von Chak, D., and Hasselbach, W. (1977) *Z. Naturforsch.* **32,** 828–834
13. Di Sabato, G., and Jencks, W. P. (1961) *J. Am. Chem. Soc.* **83,** 4400–4405
14. De Meis, L., Martins, O. B., and Alves, E. W. (1980) *Biochemistry* **19,** 4253–4261
15. Dupont, Y., and Pougeois, R. (1983) *FEBS Lett.* **156,** 93–98
16. De Meis, L., and Suzano, V. A. (1988) *FEBS Lett.* **232,** 73–77
17. De Meis, L. (1989) *Biochim. Biophys. Acta* **973,** 333–349
18. Zscherp, C., and Barth, A. (2001) *Biochemistry* **40,** 1875–1883
19. Wharton, C. W. (2000) *Nat. Prod. Rep.* **17,** 447–453
20. Mäntele, W. (1993) *Trends Biochem. Sci.* **18,** 197–202
21. Siebert, F. (1995) *Methods Enzymol.* **246,** 501–526
22. Jung, C. (2000) *J. Mol. Recognit.* **13,** 325–351
23. Gerwert, K. (1999) *Biol. Chem.* **380,** 931–935
24. Barth, A., and Zscherp, C. (2002) *Q. Rev. Biophys.* **35,** 369–430
25. Deng, H., and Callender, R. (2001) in *Infrared and Raman Spectroscopy of Biological Materials* (Gremlich, H. U., and Yan, B., eds) pp. 477–515, Marcel Dekker Inc., New York
26. Belasco, J. G., and Knowles, J. R. (1980) *Biochemistry* **19,** 472–477
27. Alben, J. O., and Caughey, W. S. (1968) *Biochemistry* **7,** 175–183
28. Barth, A., Mäntele, W., and Kreutz, W. (1990) *FEBS Lett.* **277,** 147–150
29. Barth, A., and Zscherp, C. (2000) *FEBS Lett.* **477,** 151–156
30. Kanazawa, T., and Boyer, P. D. (1973) *J. Biol. Chem.* **248,** 3163–3172
31. Barth, A., and Mäntele, W. (1998) *Biophys. J.* **75,** 538–544
32. Barth, A. (1999) *J. Biol. Chem.* **274,** 22170–22175
33. Cepus, V., Scheidig, A. J., Goody, R. S., and Gerwert, K. (1998) *Biochemistry* **37,** 10263–10271
34. Du, X., Frei, H., and Kim, S.-H. (2000) *J. Biol. Chem.* **275,** 8492–8500
35. Cheng, H., Sukal, S., Deng, H., Leyh, T. S., and Callender, R. (2001) *Biochemistry* **40,** 4035–4043
36. Barth, A. (2002) *Biopolymers* **67,** 237–241
37. Barth, A., von Germar, F., Kreutz, W., and Mäntele, W. (1996) *J. Biol. Chem.* **271,** 30637–30646
38. Deng, H., Wang, J., Callender, R., and Ray, W. J. (1998) *J. Phys. Chem. B* **1022,** 3617–3623
39. Brown, I. D., and Shannon, R. D. (1973) *Acta Crystallogr. Sect. A* **29,** 266–282
40. Brown, I. D. (2002) *The Chemical Bond in Inorganic Chemistry: The Bond Valence Model*, Oxford University Press, Oxford
41. Brown, I. D., and Wu, K. K. (1976) *Acta Crystallogr. Sect. B Struct. Crystallogr. Cryst. Chem.* **32,** 1957–1959
42. Barth, A., Kreutz, W., and Mäntele, W. (1994) *Biochim. Biophys. Acta* **1194,** 75–91
43. Barth, A., Mäntele, W., and Kreutz, W. (1991) *Biochim. Biophys. Acta* **1057,** 115–123
44. Shigekawa, M., Wakabayashi, S., and Nakamura, H. (1983) *J. Biol. Chem.* **258,** 14157–14161
45. Pauling, L. (1929) *J. Am. Chem. Soc.* **51,** 1010–1026

46. Byström, A., and Wilhelmi, K.-A. (1951) *Acta Chem. Scand.* **5,** 1003–1010
47. Brown, I. D. (1992) *Acta Crystallogr. Sect. B Struct. Crystallogr. Cryst. Chem.* **48,** 553–572
48. Layton, E. M., Kross, R. D., and Fassel, V. A. (1956) *J. Chem. Phys.* **25,** 135–138
49. Horváth, G., Illényi, J., Pusztay, L., and Simon, K. (1987) *Acta Chim. Hung.* **124,** 819–822
50. Ziólkowski, J. (1983) *J. Catal.* **84,** 317–332
51. Lehninger, A. L., Nelson, D. L., and Cox, M. M. (1993) *Principles of Biochemistry*, 2nd Ed., p. 66, Worth Publishers, New York
52. Ziólkowski, J., and Dziembaj, L. (1985) *J. Solid State Chem.* **57,** 291–299
53. Ziólkowski, J. (1985) *J. Solid State Chem.* **57,** 269–290
54. Herschbach, D. R., and Laurie, V. W. (1961) *J. Chem. Phys.* **35,** 458–463
55. Johnston, H. S. (1964) *J. Am. Chem. Soc.* **86,** 1643–1645
56. Herzberg, G. (1950) *Molecular Spectra and Molecular Structure: I. Spectra of Diatomic Molecules*, 2nd Ed., pp. 100–101, Krieger Publishing Company, Malabar
57. Gans, P. (1971) *Vibrating Molecules*, Chapman and Hall, London
58. Jencks, W. P. (1989) *Methods Enzymol.* **171,** 145–164
59. Fersht, A. (1999) *Structure and Mechanism in Protein Science*, pp. 330, 342, W. H. Freeman and Company, New York
60. Schulz, G. E., and Schirmer, R. H. (1979) *Principles of Protein Structure*, p. 28, Springer Verlag, New York
61. Murray-Rust, P., Bürgi, H.-B., and Dunitz, J. D. (1975) *J. Am. Chem. Soc.* **97,** 921–922
62. Pohle, W., Bohl, M., and Böhlig, H. (1990) *J. Mol. Struct.* **242,** 333–342
63. Narlikar, G. J., and Herschlag, D. (1997) *Annu. Rev. Biochem.* **66,** 19–59
64. Lewis, R. J., Brannigan, J. A., Muchová, K., Barák, I., and Wilkinson, A. J. (1999) *J. Mol. Biol.* **294,** 9–15
65. Cho, H., Wang, W., Kim, R., Yokota, H., Damo, S., Kim, S.-H., Wemmer, D., Kustu, S., and Yan, D. (2001) *Proc. Natl. Acad. Sci. U. S. A.* **98,** 8525–8530
66. Lahiri, S. D., Zhang, G., Dunaway-Mariano, D., and Allen, K. N. (2002) *Biochemistry* **41,** 8351–8359
67. Birck, C., Mourey, L., Gouet, P., Fabry, B., Schumacher, J., Rousseau, P., Kahn, D., and Samama, J.-P. (1999) *Structure* **7,** 1505–1515
68. Toyoshima, C., Nakasako, M., Nomura, H., and Ogawa, H. (2000) *Nature* **405,** 647–655
69. Toyoshima, C., and Nomura, H. (2002) *Nature* **418,** 605–611
70. Sigel, H., Da Costa, C. P., Song, B., Carloni, P., and Gregán, F. (1999) *J. Am. Chem. Soc.* **121,** 6248–6257
71. Herschlag, D., and Jencks, W. P. (1990) *Biochemistry* **29,** 5172–5179
72. Vilsen, B., Andersen, J. P., and MacLennan, D. H. (1991) *J. Biol. Chem.* **266,** 16157–16164
73. Sørensen, T. L., Møller, J. V., and Nissen, P. (2004) *Science* **304,** 1672–1675
74. Aravid, L., Galperin, M. Y., and Koonin, E. V. (1998) *Trends Biochem. Sci.* **4,** 127–129